Open charm spectroscopy @ LHCb

CHARM 2015, Wayne State University, Detroit

Mark Whitehead
on behalf of the LHCb collaboration

Introduction and outline

- Charm spectra well predicted by HQET
  - Important to test the predictions with measurements of mass, width and spin
  - Some deviations seen in the D_s^{**+} system – possible exotics?
  - First observations of new states

- Reminder of the D_s^{**+} spectroscopy from LHCb in 2014
  - Phys. Rev. Lett. 113 (2014) 162001, Phys. Rev. D 90 (2014) 072003

- D^{**0} spectroscopy from $B^- \to D^+ K^- \pi^-$ decays
  - Phys. Rev. D 91 (2015) 092002

- D^{**+} spectroscopy from $B^0 \to \overline{D}^0 \pi^+ \pi^-$ and $B^0 \to \overline{D}^0 K^+ \pi^-$
  - arXiv:1505.01710 and arXiv:1505.01505
  - Both submitted to PRD

NEW

LHCb experiment

VELO
Precise vertex resolution

RICH
Particle ID

HCAL
Triggering

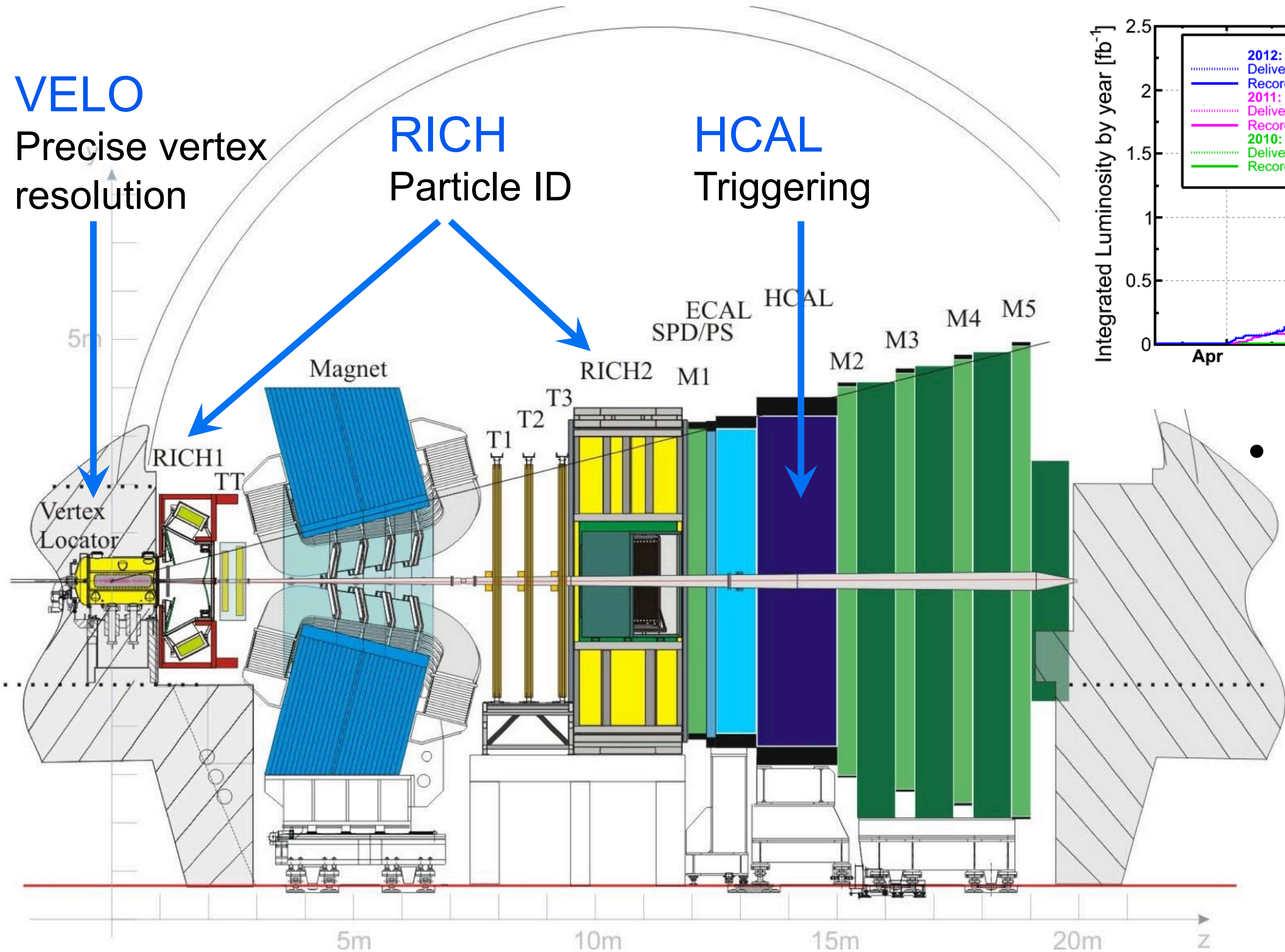

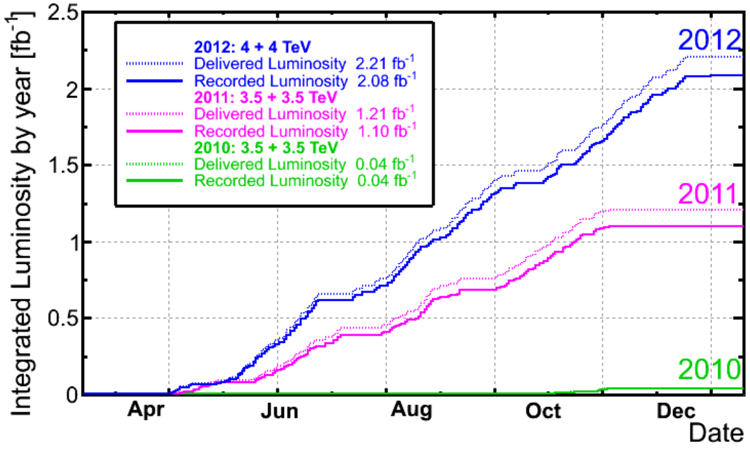

- Data samples
  - 2011 - 1fb^{-1}
  - 2012 - 2fb^{-1}
  - 3fb^{-1} combined

Dalitz plots

- Dalitz plot analysis of $B \to Dhh' \, (h, h' = K/\pi)$ decays
  - Kinematics fully constrained by particle masses

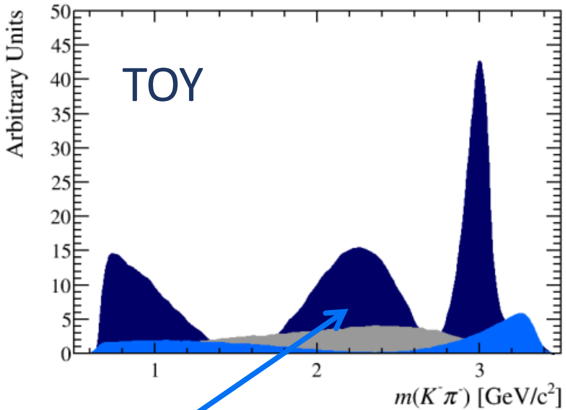

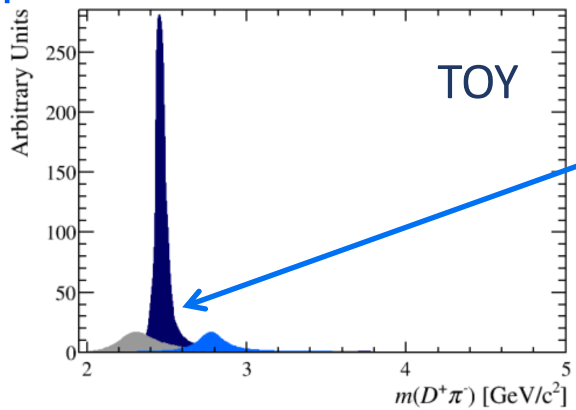

Resonances appear in invariant masses of pairs of daughters

Reflections

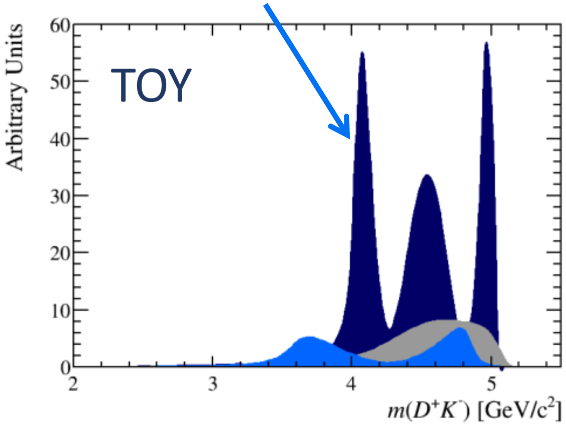

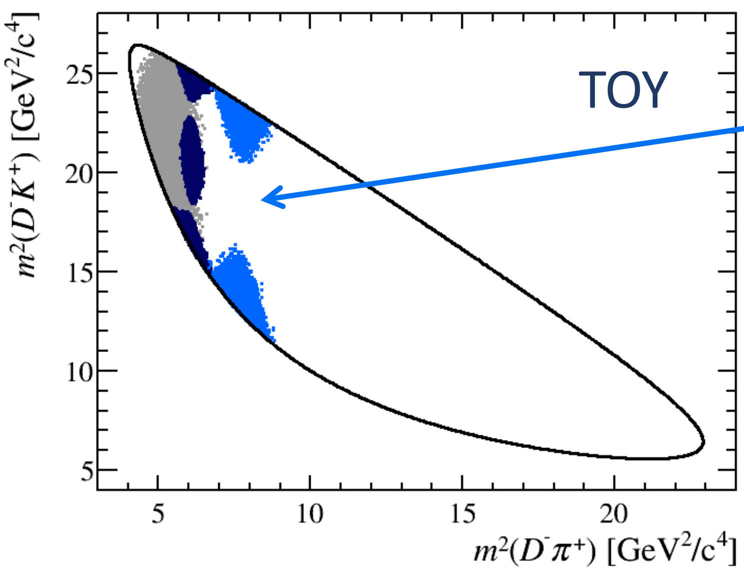

Number of gaps in a resonance band gives the spin

The Dalitz plot is the 2D representation

Charm spectroscopy

- Which charm resonances should we expect to see?
  - Only access natural spin-parity states (0^+, 1^-, 2^+…) in $B \to Dhh'$ decays

Evidence for higher mass states $D(2600)$ and $D(2760)$

Phys. Rev. D82 (2010) 111101
JHEP 09 (2013) 145

1P states measured by B-factories and LHCb

Phys. Rev. D69 (2004) 112002
Phys. Rev. D79 (2009) 112004
Phys. Rev. D82 (2010) 111101
JHEP 09 (2013) 145

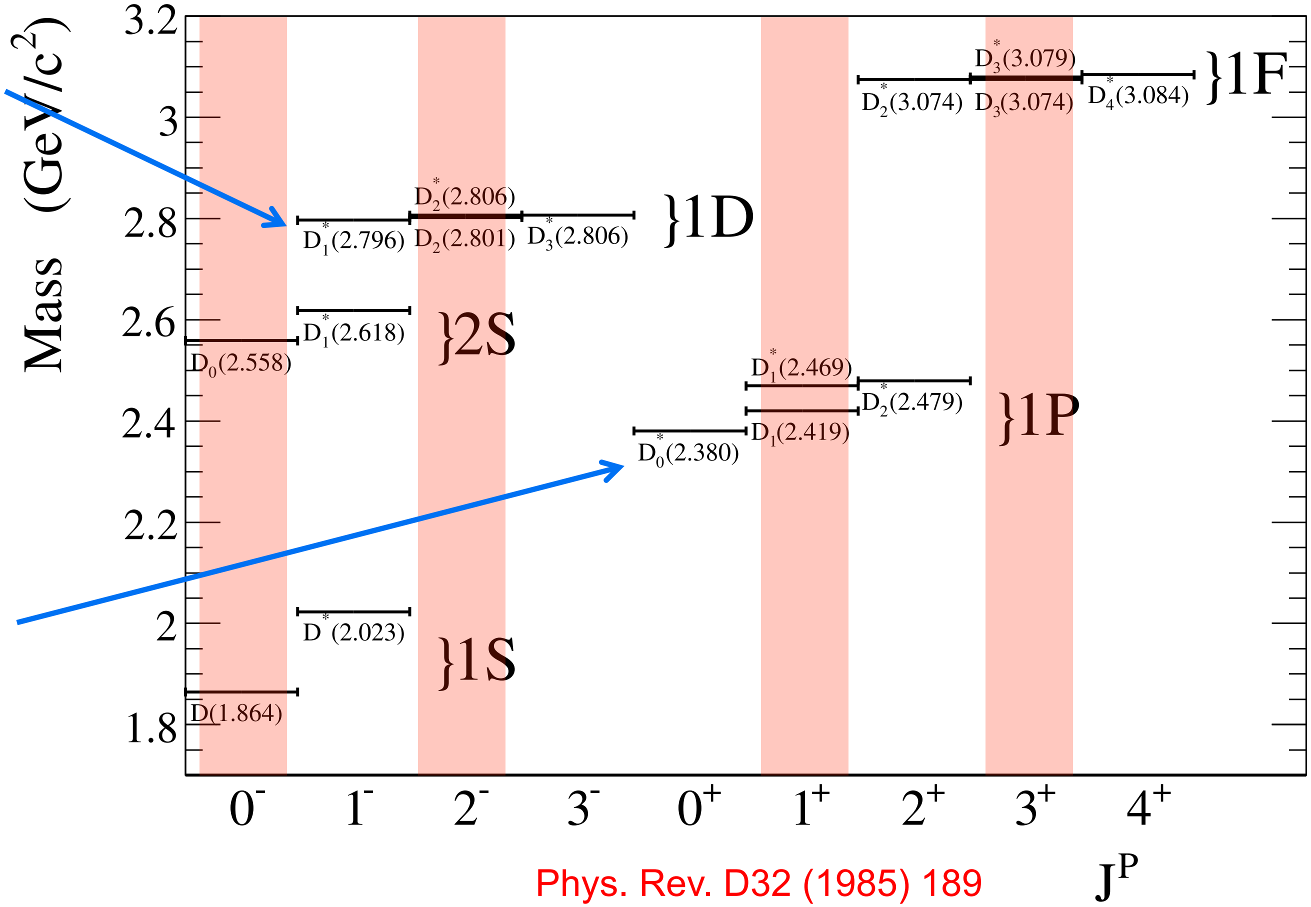

Phys. Rev. D32 (1985) 189

Charmed strange spectroscopy

Phys. Rev. Lett. 113 (2014) 162001
Phys. Rev. D 90 (2014) 072003

- What about the Ds states?
  - Full Dalitz plot analysis of $B_s^0 \to \overline{D}^0 K^- \pi^+$ decays
  - Resolved the $D_{sJ}^*(2860)^-$ state into spin 1 and spin 3 components (>10 sigma)

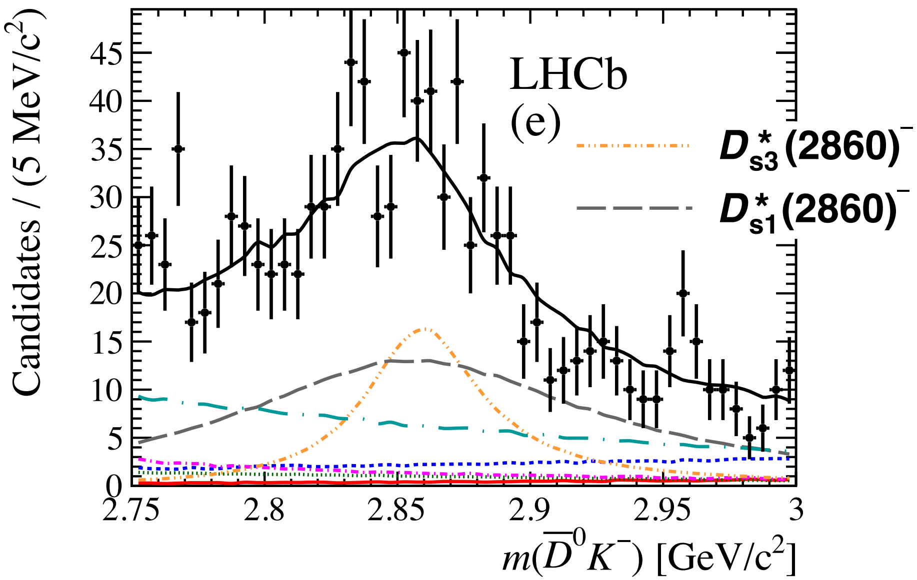

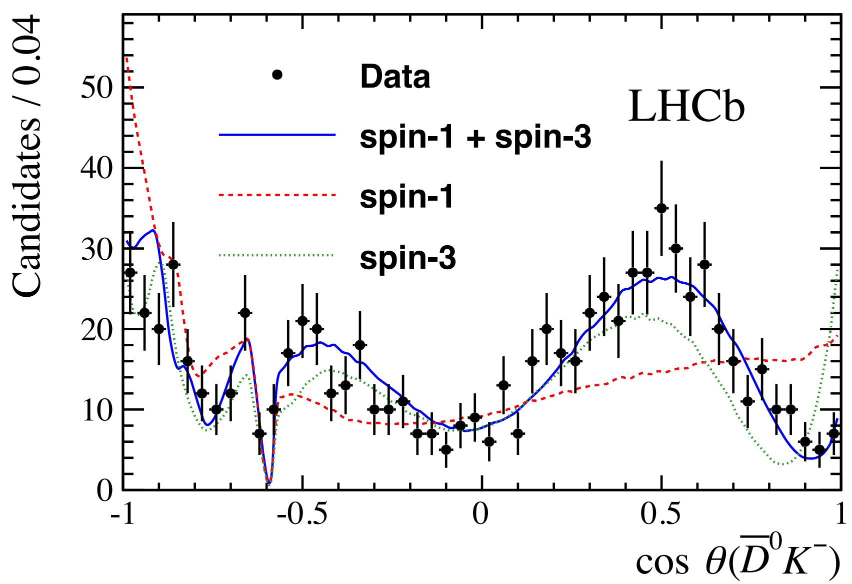

$$m(D_{s1}^*(2860)^-) = 2859 \pm 12 \pm 6 \pm 23\,\mathrm{MeV}/c^2 \qquad m(D_{s3}^*(2860)^-) = 2860.5 \pm 2.6 \pm 2.5 \pm 6.0\,\mathrm{MeV}/c^2$$
$$\Gamma(D_{s1}^*(2860)^-) = 159 \pm 23 \pm 27 \pm 72\,\mathrm{MeV}/c^2 \qquad \Gamma(D_{s3}^*(2860)^-) = 53 \pm 7 \pm 4 \pm 6\,\mathrm{MeV}/c^2\,,$$

Uncertainties are statistical, experimental systematics and model systematics

Phys. Rev. D 91 (2015) 092002

$$B^- \to D^+ K^- \pi^-$$

Analysis details – branching fraction

Phys. Rev. D 91 (2015) 092002

- Firstly observe the decay!
  - Normalise to the similar decay $B^- \to D^+\pi^-\pi^-$
  - Roughly signal 2000 candidates in the full 3 fb^{-1} data sample

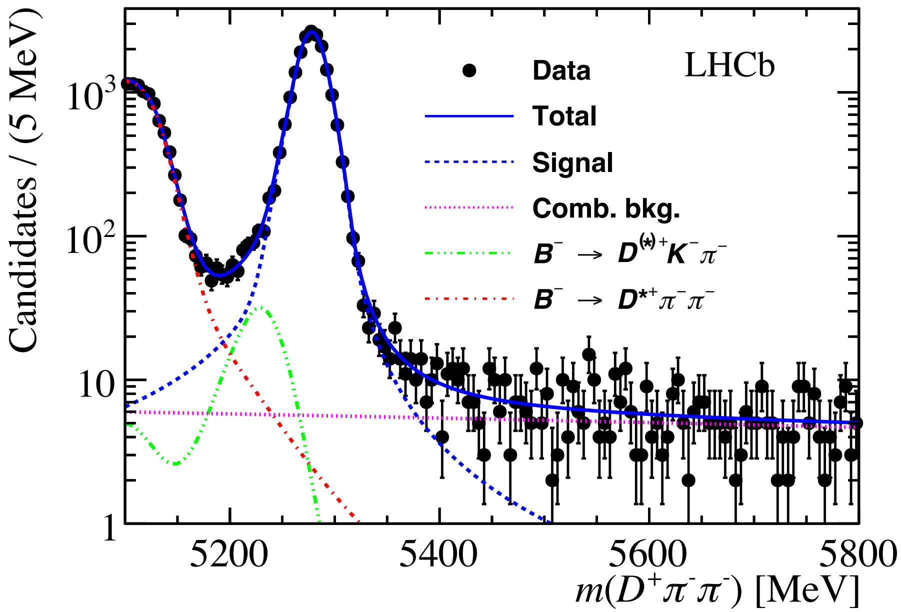

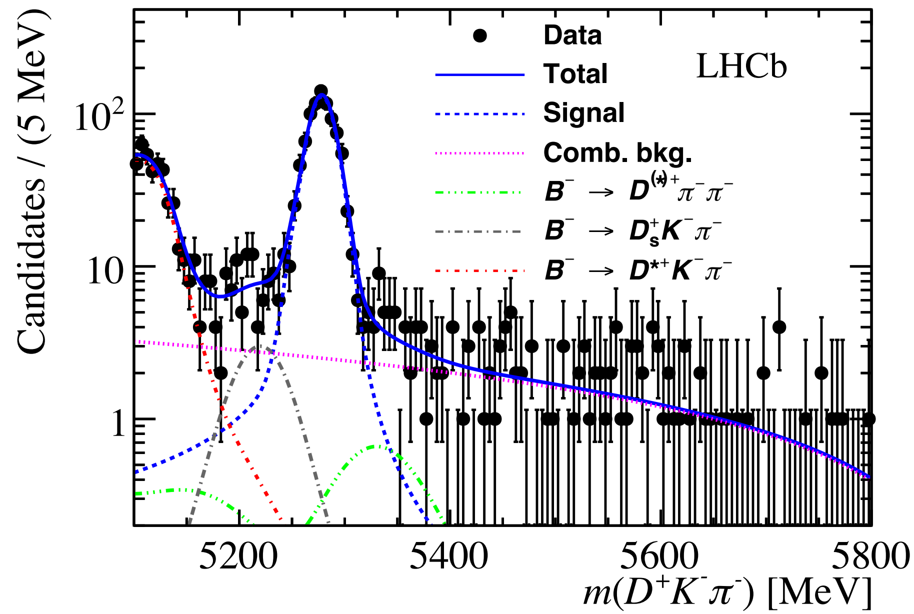

$$\mathcal{B}(B^- \to D^+K^-\pi^-) = (7.31 \pm 0.19 \pm 0.22 \pm 0.39) \times 10^{-5}$$

  - Uncertainties are statistical, systematic and from $\mathcal{B}(B^- \to D^+\pi^-\pi^-)$ (PDG)

Analysis details – DP fit

- Use mass fit to define a mass window
  - Taken as 5239.4 -> 5317.1 MeV
  - Purity in the signal region is ~93%

Phys. Rev. D 91 (2015) 092002

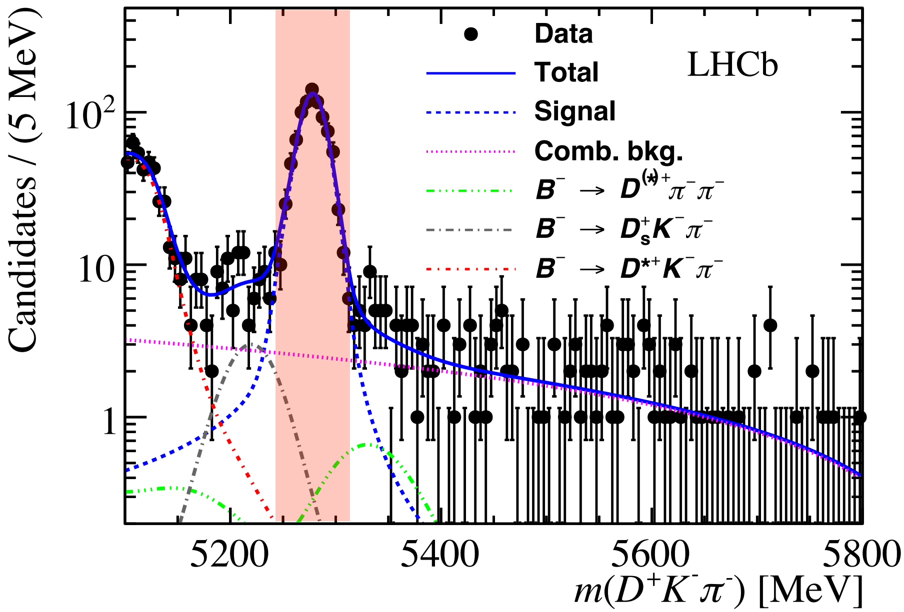

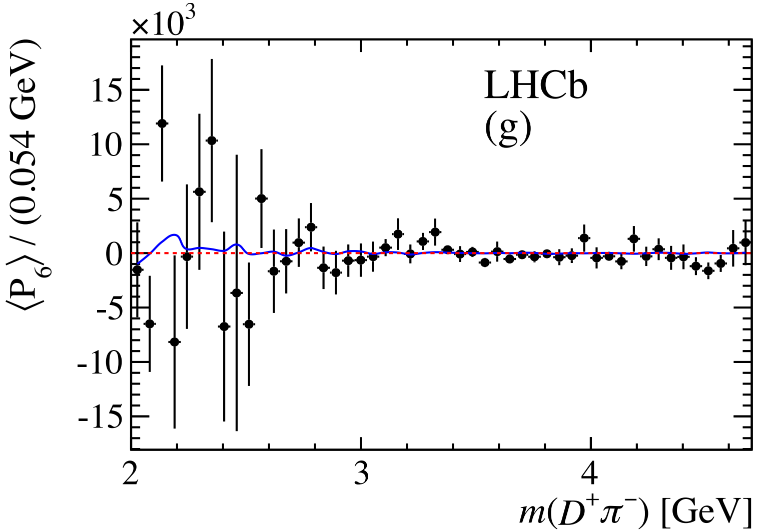

- Building the fit model
  - Only expect resonances in $m(D^+\pi^-)$
  - Angular moments from Legendre polynomials to guide the fit model
  - No evidence of structures above spin 2

Analysis details – DP model

Phys. Rev. D 91 (2015) 092002

Resonance	Spin	DP axis	Model	Parameters
$D_0^*(2400)^0$	0	$m^2(D\pi)$	RBW	$m = 2318 \pm 29\,\text{MeV},\ \Gamma = 267 \pm 40\,\text{MeV}$
$D_2^*(2460)^0$	2	$m^2(D\pi)$	RBW	Determined from data
$D_J^*(2760)^0$	1	$m^2(D\pi)$	RBW	
Nonresonant	0	$m^2(D\pi)$	EFF	Determined from data
Nonresonant	1	$m^2(D\pi)$	EFF	
$D_v^*(2007)^0$	1	$m^2(D\pi)$	RBW	$m = 2006.98 \pm 0.15\,\text{MeV},\ \Gamma = 2.1\,\text{MeV}$
B_v^{*0}	1	$m^2(DK)$	RBW	$m = 5325.2 \pm 0.4\,\text{MeV},\ \Gamma = 0.0\,\text{MeV}$

RBW = Relativistic Breit-Wigner and EFF = Exponential form factor

- Nominal model
  - Three resonances, two nonresonant terms and two virtual states
  - Efficiencies and backgrounds modelled in the fit
  - Fit performed with the Laura++ package using the Isobar model

http://laura.hepforge.org

Results

Phys. Rev. D 91 (2015) 092002

- $D_J^*(2760)^0$ state favours spin 1
  - Other hypotheses rejected with high significance (>6 sigma)
  - Mass and widths reported
  - Full results of the amplitude fit in the back-ups

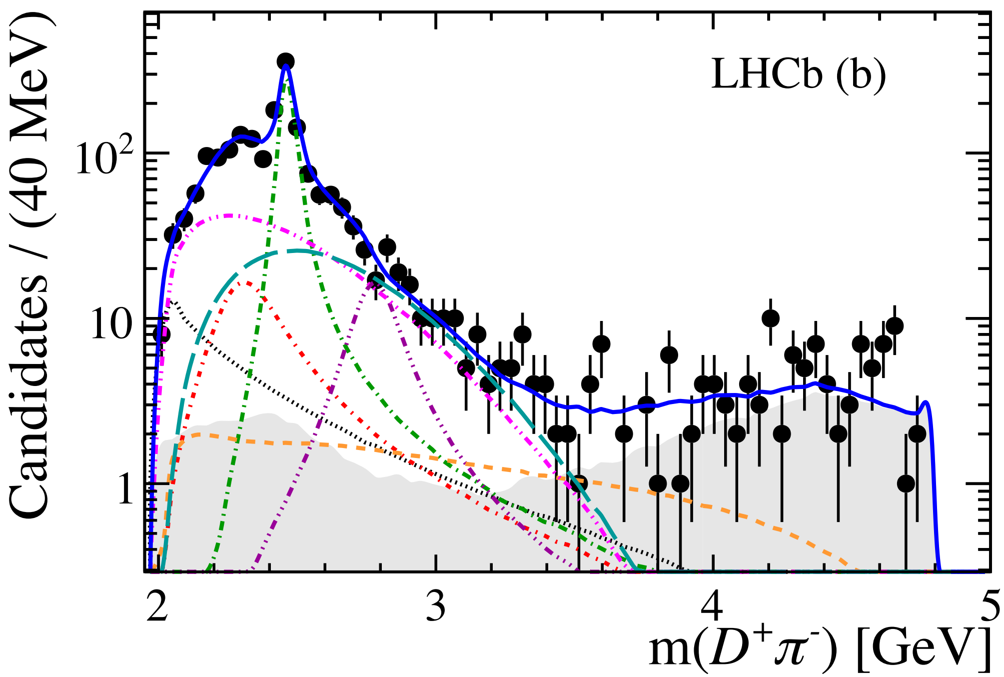

$$
\begin{aligned}
m(D_2^*(2460)^0) &= (2464.0 \pm 1.4 \pm 0.5 \pm 0.2)\ \mathrm{MeV} \\
\Gamma(D_2^*(2460)^0) &= (43.8 \pm 2.9 \pm 1.7 \pm 0.6)\ \mathrm{MeV} \\
m(D_1^*(2760)^0) &= (2781 \pm 18 \pm 11 \pm 6)\ \mathrm{MeV} \\
\Gamma(D_1^*(2760)^0) &= (177 \pm 32 \pm 20 \pm 7)\ \mathrm{MeV}
\end{aligned}
$$

Uncertainties are statistical, experimental systematics and model systematics

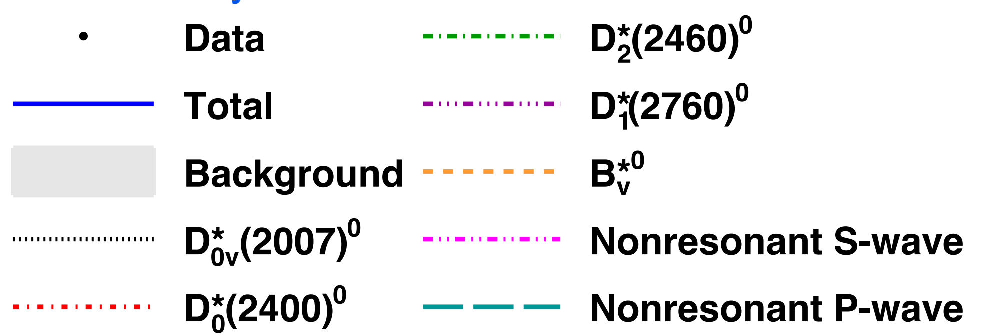

arXiv:1505.01710

$$B^0 \to \overline{D}^0 \pi^+ \pi^-$$

Analysis details – mass fit

arXiv:1505.01710

- Full amplitude analysis of $B^0 \to \overline{D}^0 \pi^+ \pi^-$ decays
  - Expect resonances in $m(\pi^+\pi^-)$ and $m(\overline{D}^0\pi^-)$
  - Use only $\overline{D}^0 \to K^+\pi^-$
- Firstly perform a mass fit to select events for DP fit
  - Combinatorial background removed with Fisher discriminant MVA
  - ~10000 signal candidates (in 3 fb^{-1})
  - Signal region 5250 – 5310 MeV/c^2
  - Purity of ~98% in the signal window

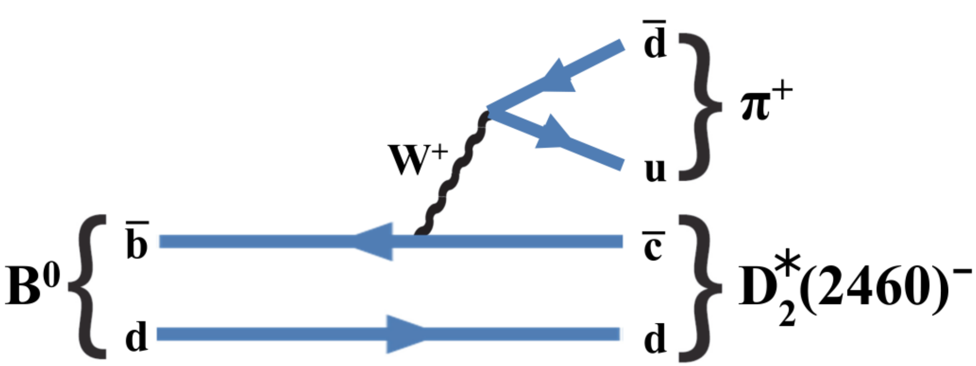

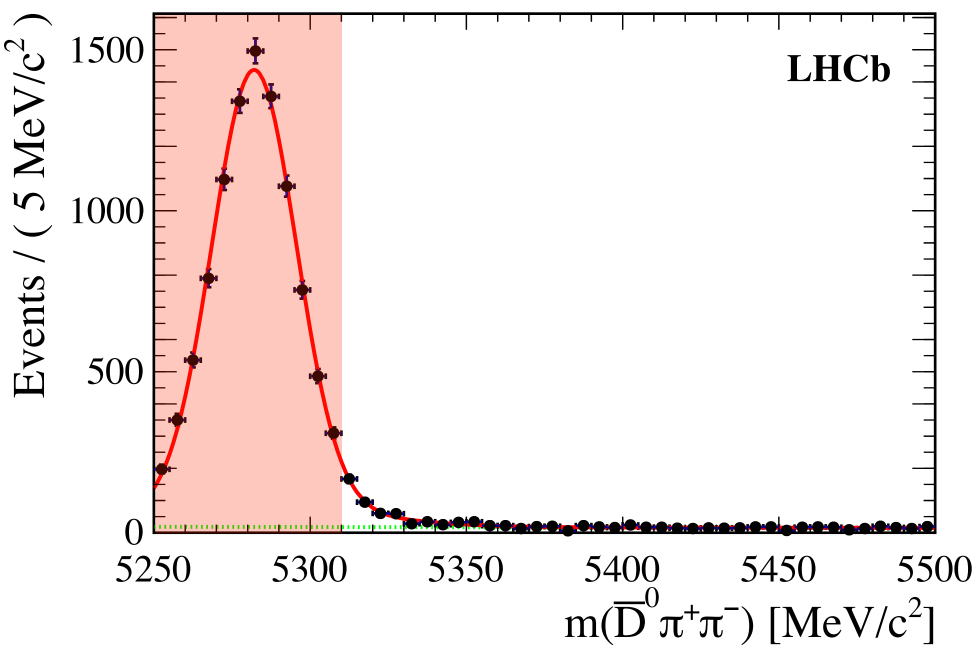

Analysis details – DP model

arXiv:1505.01710

- Two DP fit models to choose from
  - Isobar model and K-matrix parameterisations of the ππ S-wave

- Isobar model
  - 11 resonances
  - Two nonresonant terms

- K-matrix model
  - Eight resonances
  - 1 non resonant term
  - K-matrix term

Resonance	Spin	Model	m_r (MeV/c^2)	Γ_0 (MeV)
$\overline{D}^0\pi^-$ P-wave	1	Eq. 14	Floated	
$D_0^*(2400)^-$	0	RBW	Floated	
$D_2^*(2460)^-$	2	RBW	Floated	
$D_J^*(2760)^-$	3	RBW	Floated	
$\rho(770)$	1	GS	775.02 ± 0.35	149.59 ± 0.67
$\omega(782)$	1	Eq. 13	781.91 ± 0.24	8.13 ± 0.45
$\rho(1450)$	1	GS	1493 ± 15	427 ± 31
$\rho(1700)$	1	GS	1861 ± 17	316 ± 26
$f_2(1270)$	2	RBW	1275.1 ± 1.2	$185.1\,^{+2.9}_{-2.4}$
$\pi\pi$ S-wave	0	K-matrix		
$f_0(500)$	0	Eq. 15		
$f_0(980)$	0	Eq. 18		
$f_0(2020)$	0	RBW	1992 ± 16	442 ± 60
Nonresonant	0	Eq. 20		

RBW = Relativistic Breit-Wigner and GS = Gounaris-Sakurai. Listed eqs. are in the backup slides

Analysis details – DP fit

arXiv:1505.01710

- Plots from the Isobar model fit
  - K-matrix plots in the back-ups
  - Bump seen in $m(\overline{D}^0\pi^-)$ at 2760 MeV/c²
  - Rich structure also in $m(\pi^+\pi^-)$
  - Good agreement between models

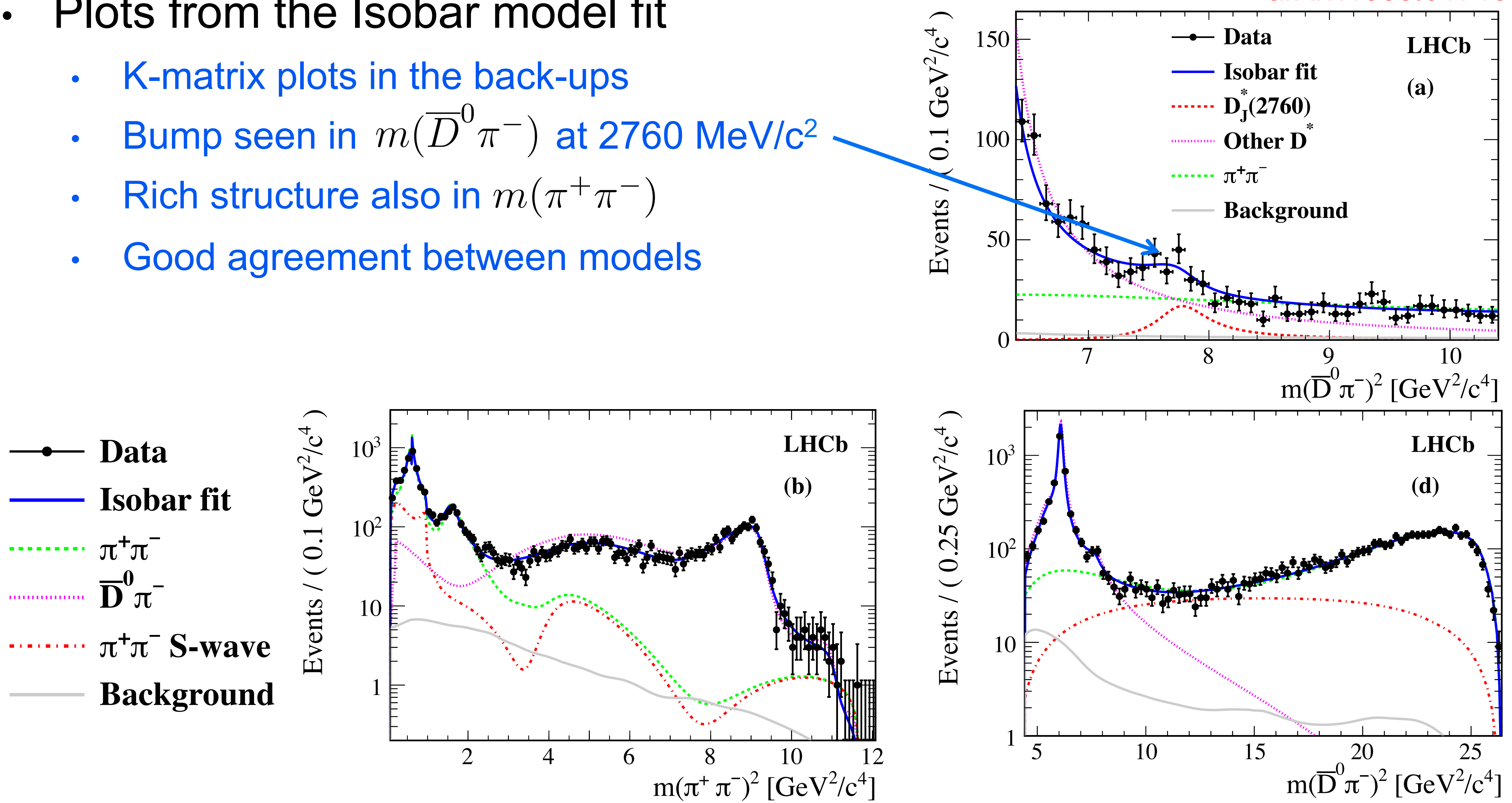

Analysis details – results

arXiv:1505.01710

- $D_J^*(2760)^-$ determined to be spin 3
  - Other spins ruled out by at least 10 sigma
  - No evidence for an additional spin-1 state

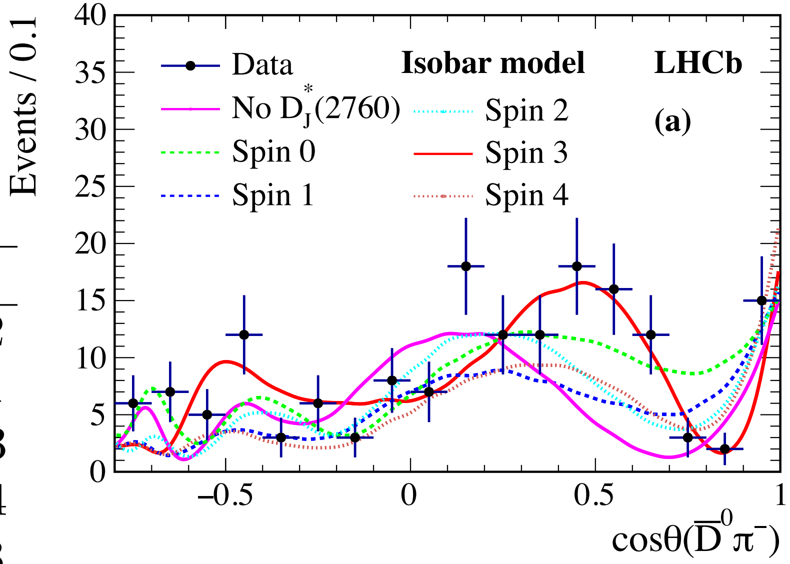

		Isobar	K-matrix
$D_0^*(2400)$	m	$2349 \pm 6 \pm 1 \pm 4$	$2354 \pm 7 \pm 11 \pm 2$
	Γ	$217 \pm 13 \pm 5 \pm 12$	$230 \pm 15 \pm 18 \pm 11$
$D_2^*(2460)$	m	$2468.6 \pm 0.6 \pm 0.0 \pm 0.3$	$2468.1 \pm 0.6 \pm 0.4 \pm 0.3$
	Γ	$47.3 \pm 1.5 \pm 0.3 \pm 0.6$	$46.0 \pm 1.4 \pm 1.7 \pm 0.4$
$D_3^*(2760)$	m	$2798 \pm 7 \pm 1 \pm 7$	$2802 \pm 11 \pm 10 \pm 3$
	Γ	$105 \pm 18 \pm 6 \pm 23$	$154 \pm 27 \pm 13 \pm 9$

Uncertainties are statistical, experimental systematics and model systematics

- See back-ups for further (non-spectroscopy) results
  - Branching fraction measurements
  - Amplitude fit parameters

arXiv:1505.01505

$$B^0 \to \overline{D}^0 K^+ \pi^-$$

Analysis details

arXiv:1505.01505

- Full amplitude analysis of $B^0 \to \overline{D}^0 K^+\pi^-$ decays
  - Expect resonances in $m(K^+\pi^-)$ and $m(\overline{D}^0\pi^-)$
  - Use only $\overline{D}^0 \to K^+\pi^-$
  - Access to the same charm resonances as $B^0 \to \overline{D}^0\pi^+\pi^-$ but lower statistics
  - Most interesting for a future measurement of the CKM angle gamma

- Mass fit to select events for DP fit
  - Roughly 2500 signal candidates
  - Uses the full 3 fb^{-1} data sample
  - Signal window 5248.55 – 5309.05 MeV
  - Purity ~75% in the signal region

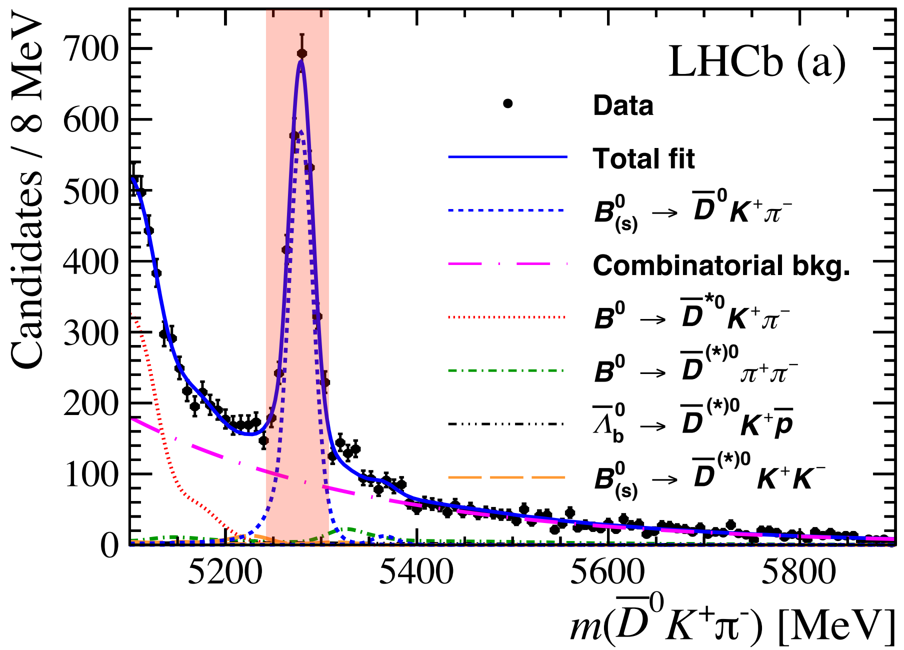

Analysis details – DP fit

arXiv:1505.01505

- Nominal Amplitude model
  - Five resonant terms, two nonresonant components and the LASS shape
  - Backgrounds and efficiency variation over the DP included
  - The Laura++ package was used to perform the amplitude fit http://laura.hepforge.org
  - Isobar formalism used

Resonance	Spin	DP axis	Model	Parameters
$K^*(892)^0$	1	$m^2(K^+\pi^-)$	RBW	$m_0 = 895.81 \pm 0.19\,\text{MeV},\ \Gamma_0 = 47.4 \pm 0.6\,\text{MeV}$
$K^*(1410)^0$	1	$m^2(K^+\pi^-)$	RBW	$m_0 = 1414 \pm 15\,\text{MeV},\ \Gamma_0 = 232 \pm 21\,\text{MeV}$
$K_0^*(1430)^0$	0	$m^2(K^+\pi^-)$	LASS	Determined from data
$K_2^*(1430)^0$	2	$m^2(K^+\pi^-)$	RBW	$m_0 = 1432.4 \pm 1.3\,\text{MeV},\ \Gamma_0 = 109 \pm 5\,\text{MeV}$
$D_0^*(2400)^-$	0	$m^2(\overline{D}^0\pi^-)$	RBW	Determined from data
$D_2^*(2460)^-$	2	$m^2(\overline{D}^0\pi^-)$	RBW	
Nonresonant	0	$m^2(\overline{D}^0\pi^-)$	dabba	Fixed
Nonresonant	1	$m^2(\overline{D}^0\pi^-)$	EFF	Determined from data

RBW = Relativistic Breit-Wigner, EFF = Exponential form factor. For dabba and LASS see back-ups

Analysis details – results

- No evidence of $D_J^*(2760)^-$ contribution
  - No significant spin 1 or 3 state
  - More data required in run 2
  - See back-ups for further results

$$
\begin{aligned}
m(D_0^*(2400)^-) &= (2360 \pm 15 \pm 12 \pm 28)\ \mathrm{MeV} \\
\Gamma(D_0^*(2400)^-) &= (255 \pm 26 \pm 20 \pm 47)\ \mathrm{MeV} \\
m(D_2^*(2460)^-) &= (2465.6 \pm 1.8 \pm 0.5 \pm 1.2)\ \mathrm{MeV} \\
\Gamma(D_2^*(2460)^-) &= (46.0 \pm 3.4 \pm 1.4 \pm 2.9)\ \mathrm{MeV}
\end{aligned}
$$

Uncertainties are statistical, experimental systematics and model systematics

arXiv:1505.01505

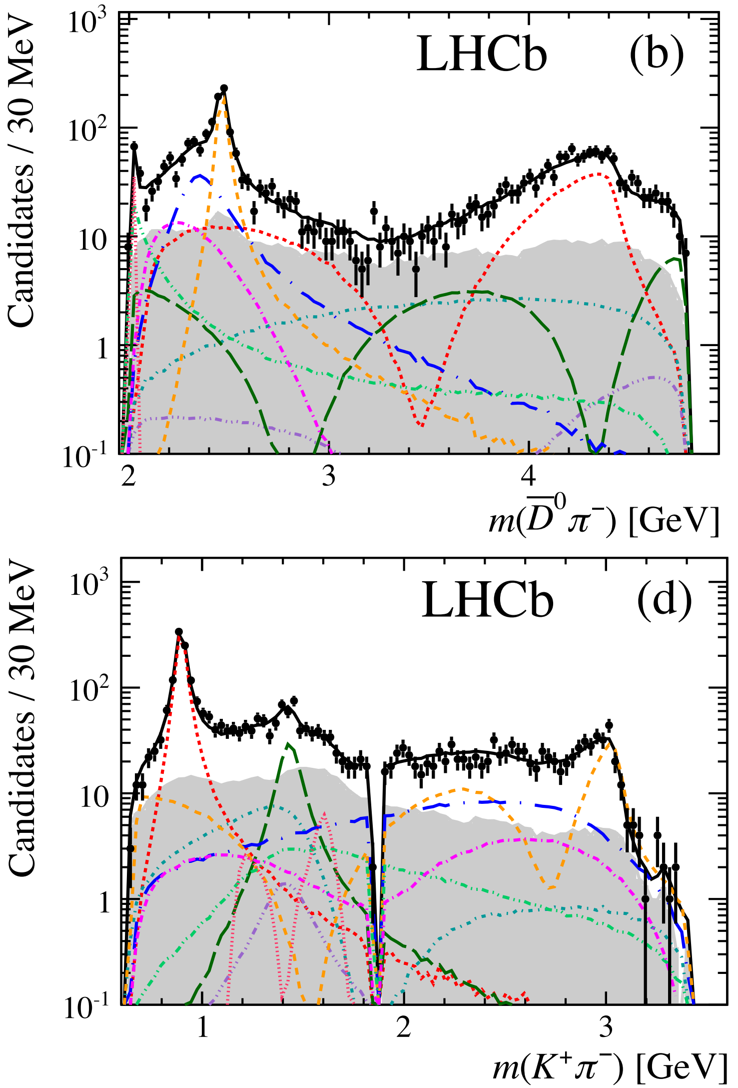

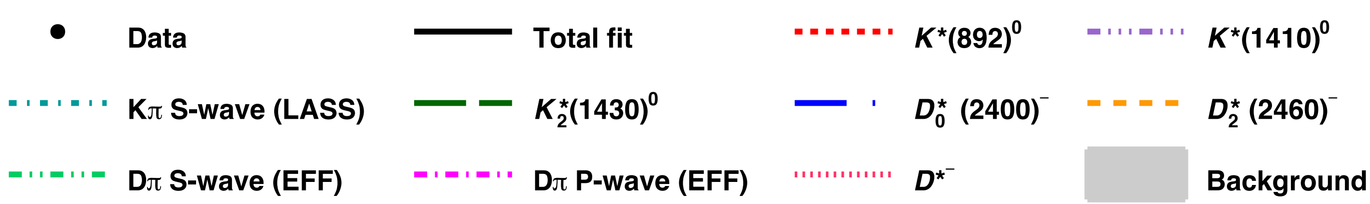

Summary

- Three amplitude analyses of $B \to Dhh'$ decays performed
  - $D_J^*(2760)^0$ determined to be spin 1 for the first time
  - $D_J^*(2760)^-$ determined to be spin 3 for the first time
  - Interesting to see how this develops – recall spin 1 and spin 3 in D_s^{**+} system
  - Several worlds most precise measurements of masses and widths

- Full results of these analyses in the back-ups
  - Branching fraction measurements
  - Parameters from the amplitude fits

- Look out for future charm spectroscopy from LHCb

Back-up

$B^- \to D^+ K^- \pi^-$

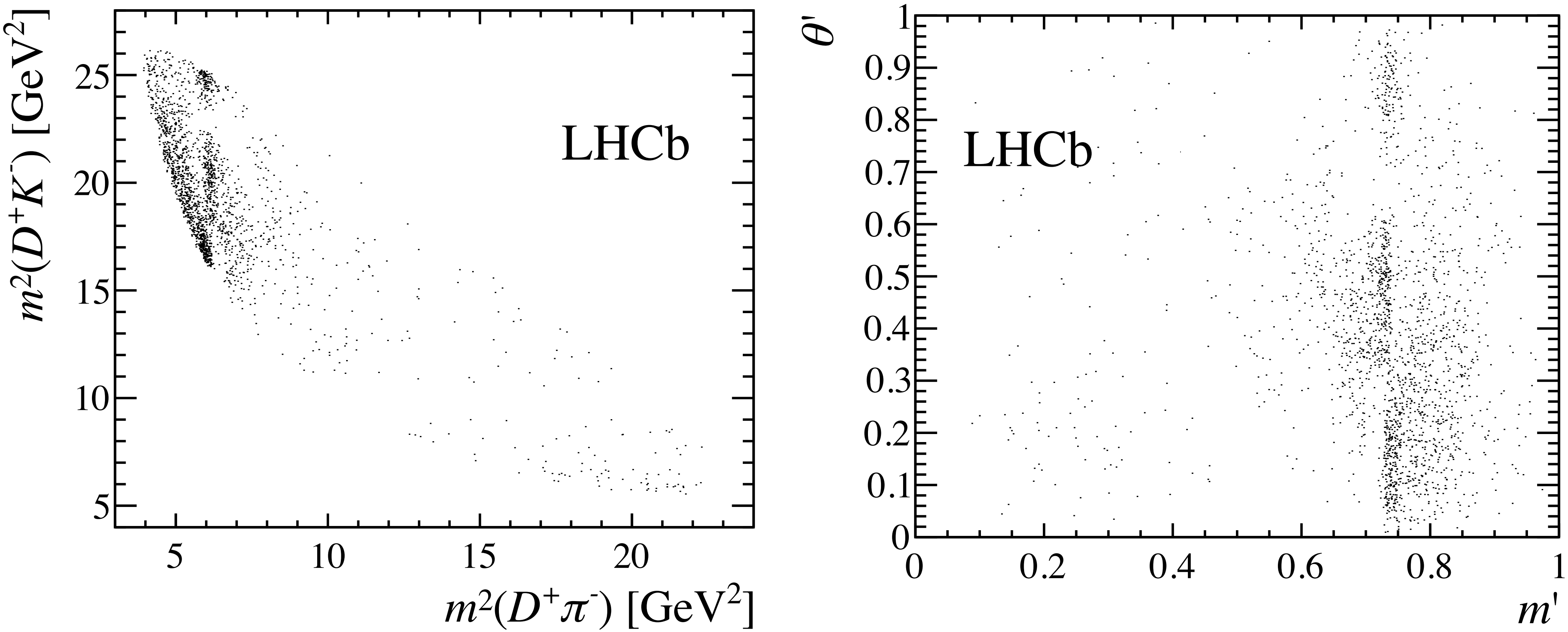
LHCb
$m^2(D^+K^-)$ [GeV^2]
$m^2(D^+\pi^-)$ [GeV^2]
5
10
15
20
25
LHCb
θ'
m'
0
0.1
0.2
0.3
0.4
0.5
0.6
0.7
0.8
0.9
1

$$B^- \to D^+ K^- \pi^-$$

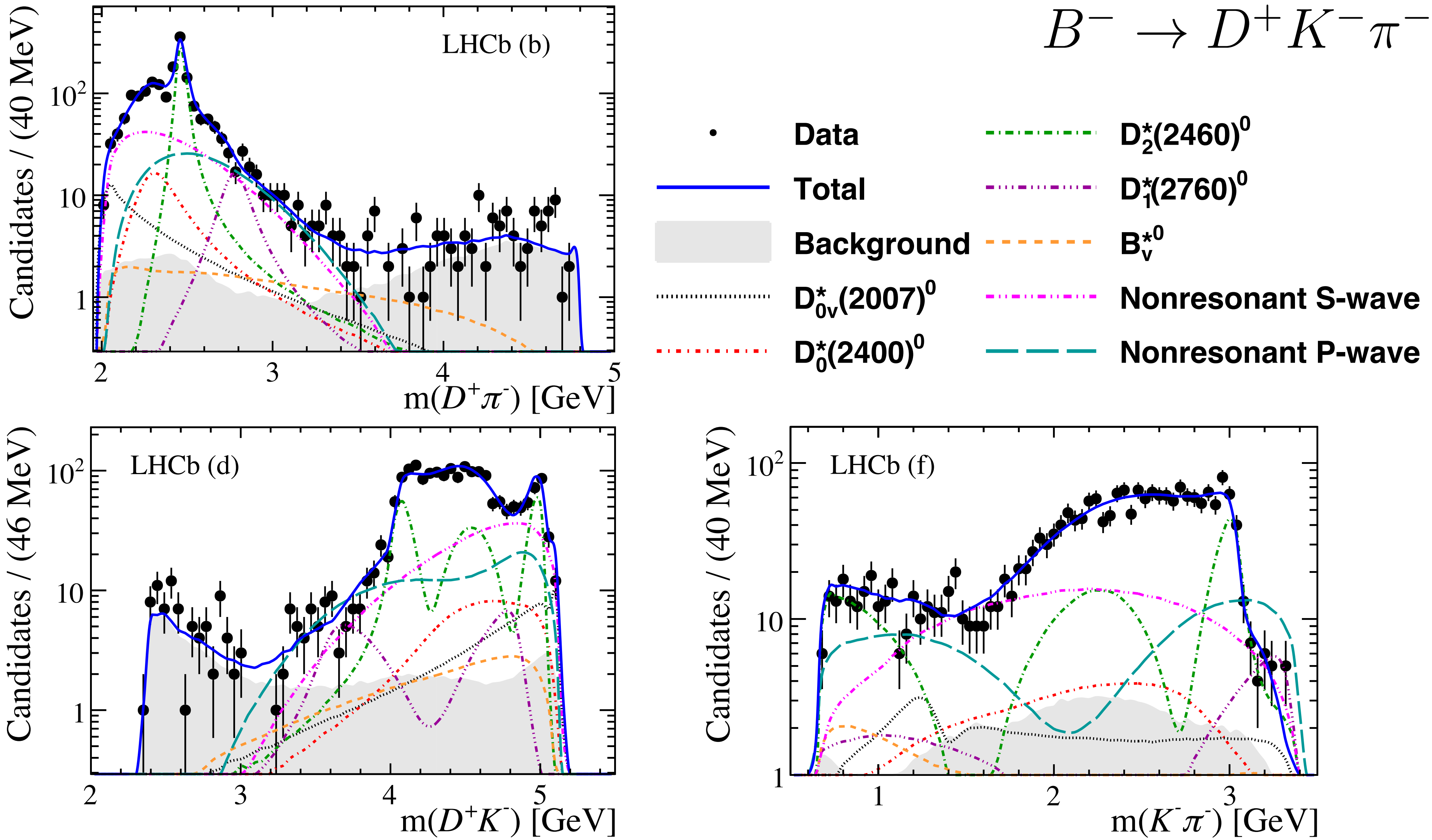
LHCb (b)
Candidates / (40 MeV)
m($D^+\pi^-$) [GeV]
Data
Total
Background
$D^*_{0v}(2007)^0$
$D^*_0(2400)^0$
$D^*_2(2460)^0$
$D^*_1(2760)^0$
B^{*0}_v
Nonresonant S-wave
Nonresonant P-wave
LHCb (d)
Candidates / (46 MeV)
m(D^+K^-) [GeV]
LHCb (f)
Candidates / (40 MeV)
m($K^-\pi^-$) [GeV]

$B^- \to D^+ K^- \pi^-$

Table 12: Results for the complex amplitudes and their uncertainties. The three quoted errors are statistical, experimental systematic and model uncertainties, respectively.

	Isobar model coefficients	
Resonance	Real part	Imaginary part
$D_0^*(2400)^0$	$-0.04 \pm 0.07 \pm 0.03 \pm 0.28$	$-0.51 \pm 0.07 \pm 0.02 \pm 0.13$
$D_2^*(2460)^0$	1.00	0.00
$D_1^*(2760)^0$	$-0.32 \pm 0.06 \pm 0.03 \pm 0.03$	$-0.23 \pm 0.07 \pm 0.03 \pm 0.03$
S-wave nonresonant	$0.93 \pm 0.09 \pm 0.03 \pm 0.17$	$-0.58 \pm 0.08 \pm 0.03 \pm 0.15$
P-wave nonresonant	$-0.43 \pm 0.09 \pm 0.03 \pm 0.34$	$0.75 \pm 0.09 \pm 0.05 \pm 0.68$
$D_v^*(2007)^0$	$0.16 \pm 0.08 \pm 0.03 \pm 0.56$	$0.46 \pm 0.09 \pm 0.04 \pm 0.77$
B_v^*	$-0.07 \pm 0.08 \pm 0.22 \pm 0.09$	$0.33 \pm 0.07 \pm 0.02 \pm 0.08$

Table 13: Results for the complex amplitudes and their uncertainties. The three quoted errors are statistical, experimental systematic and model uncertainties, respectively.

	Isobar model coefficients	
Resonance	Magnitude	Phase
$D_0^*(2400)^0$	$0.51 \pm 0.09 \pm 0.02 \pm 0.15$	$-1.65 \pm 0.16 \pm 0.06 \pm 0.50$
$D_2^*(2460)^0$	1.00	0.00
$D_1^*(2760)^0$	$0.39 \pm 0.05 \pm 0.01 \pm 0.03$	$-2.53 \pm 0.24 \pm 0.08 \pm 0.08$
S-wave nonresonant	$1.09 \pm 0.09 \pm 0.02 \pm 0.20$	$-0.56 \pm 0.09 \pm 0.04 \pm 0.11$
P-wave nonresonant	$0.87 \pm 0.09 \pm 0.03 \pm 0.11$	$2.09 \pm 0.15 \pm 0.05 \pm 0.95$
$D_v^*(2007)^0$	$0.49 \pm 0.07 \pm 0.04 \pm 0.05$	$1.24 \pm 0.17 \pm 0.07 \pm 0.60$
B_v^*	$0.34 \pm 0.06 \pm 0.03 \pm 0.07$	$1.78 \pm 0.23 \pm 0.11 \pm 0.27$

$B^- \to D^+ K^- \pi^-$

Table 15: Results for the product branching fractions $\mathcal{B}(B^- \to RK^-) \times \mathcal{B}(R \to D^+\pi^-)$ (10^{-4}). The four quoted errors are statistical, experimental systematic, model and inclusive branching fraction uncertainties, respectively.

Resonance	Branching fraction
$D_0^*(2400)^0$	$6.1 \pm 1.9 \pm 0.5 \pm 1.4 \pm 0.4$
$D_2^*(2460)^0$	$23.2 \pm 1.1 \pm 0.6 \pm 1.0 \pm 1.6$
$D_1^*(2760)^0$	$3.6 \pm 0.9 \pm 0.3 \pm 0.7 \pm 0.2$
S-wave nonresonant	$27.8 \pm 5.4 \pm 1.1 \pm 7.9 \pm 1.9$
P-wave nonresonant	$17.4 \pm 4.1 \pm 1.5 \pm 2.7 \pm 1.2$
$D_v^*(2007)^0$	$5.6 \pm 1.7 \pm 1.0 \pm 1.1 \pm 0.4$
B_v^*	$2.6 \pm 1.4 \pm 0.6 \pm 1.2 \pm 0.2$

$$B^0 \to \overline{D}^0 \pi^+ \pi^-$$

The $\rho - \omega$ interference is taken into account by

$$R_{\rho-\omega}(s) = \mathrm{GS}_{\rho(770)}(s) \times (1 + ae^{i\theta}\mathrm{RBW}_{\omega(782)}(s)), \tag{13}$$

where Γ_0 is used, instead of the mass-dependent width $\Gamma^{(L)}(s)$, for $\omega(782)$ [82].

$$R_{f_0(500)}(s) = m_r\Gamma_1(s) / \left[m_r^2 - s - g_1^2 \frac{s - s_A}{m_r^2 - s_A} z(s) - im_r\Gamma_{\mathrm{tot}}(s)\right], \tag{15}$$

The Flatté formula [84] is used to describe the $f_0(980)$ lineshape,

$$R_{f_0(980)}(s) = \frac{1}{m_r^2 - s - im_r(\rho_{\pi\pi}(s)g_1 + \rho_{KK}(s)g_2)}, \tag{18}$$

The nonresonant contribution is described by

$$R_{NR}(m^2(\pi^+\pi^-), m^2(\overline{D}^0\pi^+)) = e^{i\alpha m^2(\pi^+\pi^-)}. \tag{20}$$

Its modulus equals unity, and a slowly varying phase over $m^2(\pi^+\pi^-)$ accounts for rescattering effects of the $\pi^+\pi^-$ final state and α is a free parameter of the model.

$B^0 \to \overline{D}^0 \pi^+ \pi^-$

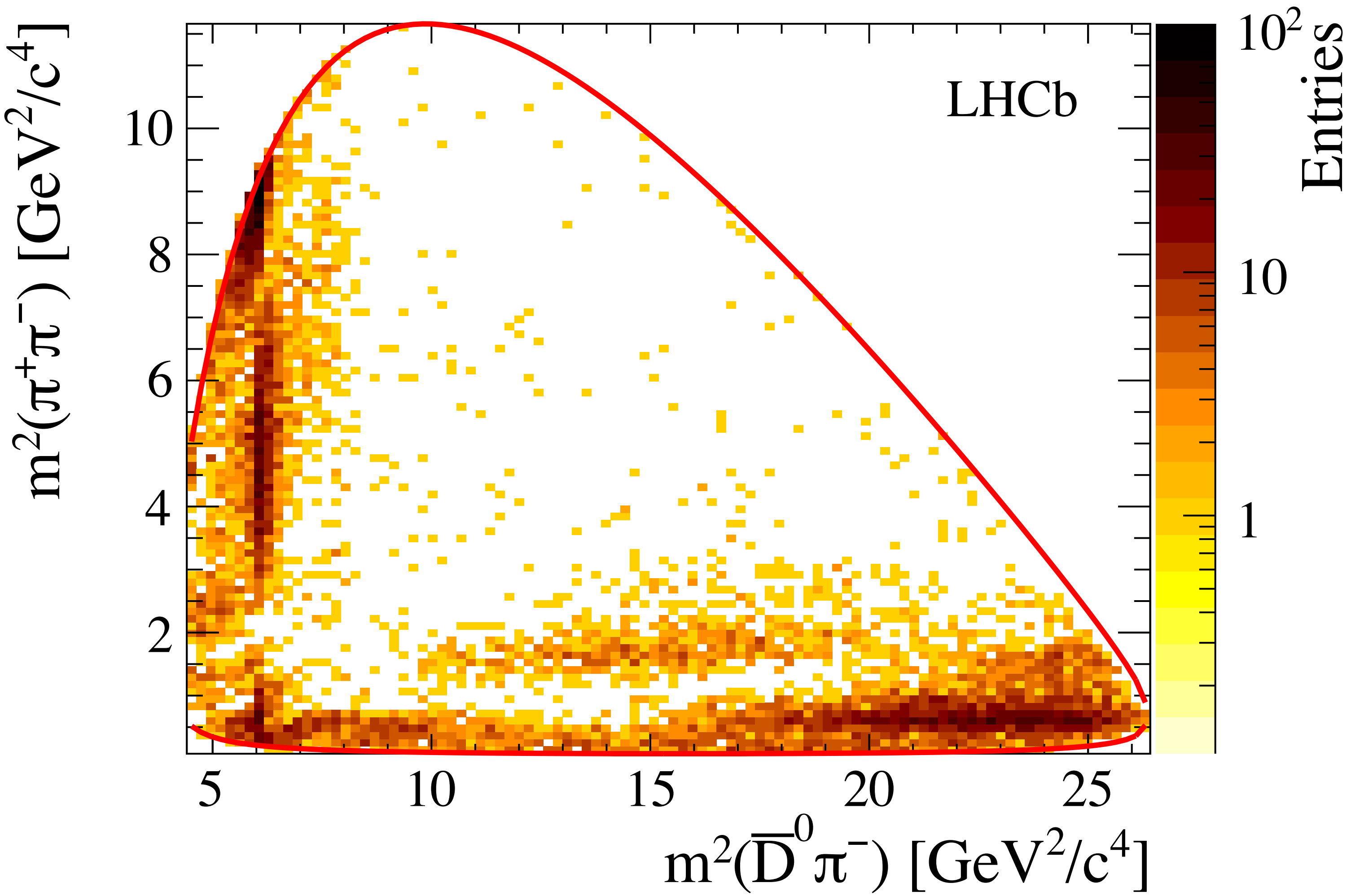

$$B^0 \to \overline{D}^0 \pi^+ \pi^-$$

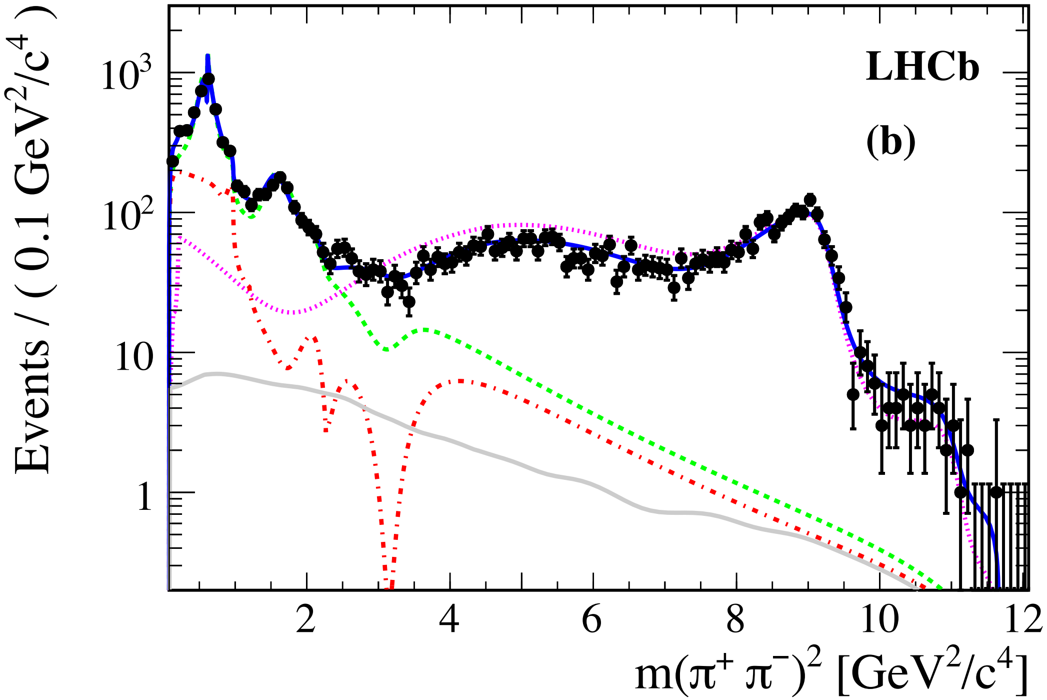

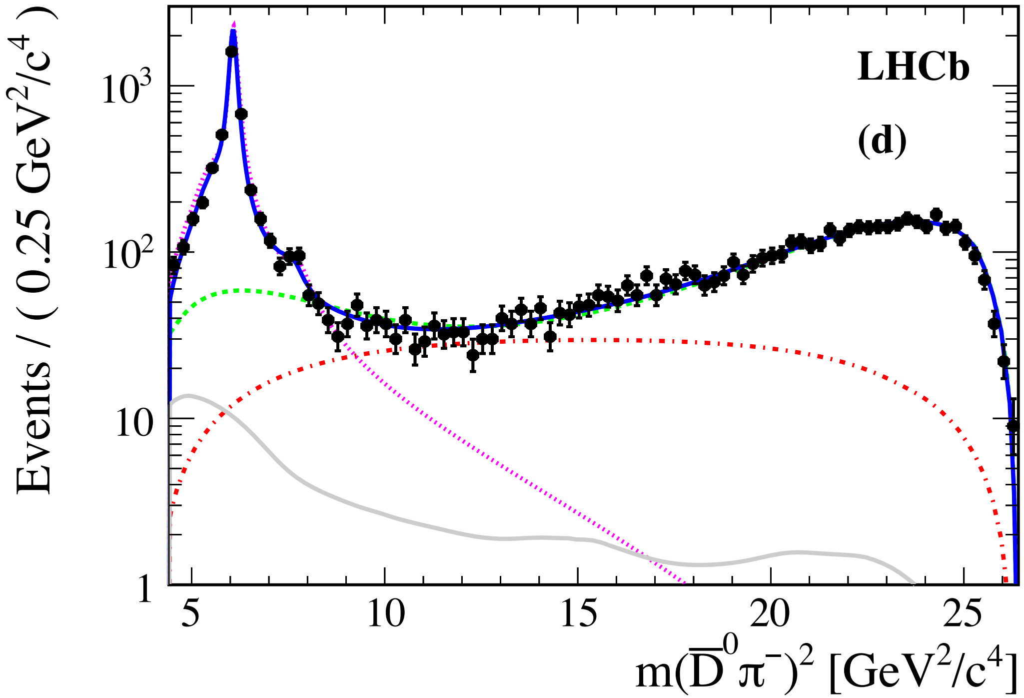

$B^0 \to \overline{D}^0 \pi^+ \pi^-$

Table 7: The moduli of the complex coefficients of the resonant contributions for the Isobar model and the K-matrix model. The first uncertainty is statistical, the second and the third are experimental and model-dependent systematic uncertainties, respectively.

Resonance	Isobar ($\lvert c_i \rvert$)	K-matrix ($\lvert c_i \rvert$)
Nonresonance	$3.43 \pm 0.22 \pm 0.04 \pm 0.51$	n/a
$f_0(500)$	$18.7 \pm 0.70 \pm 0.29 \pm 0.80$	n/a
$f_0(980)$	$2.62 \pm 0.25 \pm 0.09 \pm 0.46$	n/a
$f_0(2020)$	$4.41 \pm 0.51 \pm 0.21 \pm 1.78$	n/a
$\rho(770)$	1.0 (fixed)	1.0 (fixed)
$\omega(782)$	$0.30 \pm 0.04 \pm 0.00 \pm 0.01$	$0.31 \pm 0.04 \pm 0.01 \pm 0.01$
$\rho(1450)$	$0.23 \pm 0.03 \pm 0.01 \pm 0.02$	$0.28 \pm 0.03 \pm 0.08 \pm 0.01$
$\rho(1700)$	$0.078 \pm 0.016 \pm 0.006 \pm 0.008$	$0.136 \pm 0.020 \pm 0.077 \pm 0.011$
$f_2(1270)$	$0.072 \pm 0.002 \pm 0.000 \pm 0.005$	$0.073 \pm 0.002 \pm 0.006 \pm 0.003$
$\overline{D}^0\pi^-$ P-wave	$18.8 \pm 0.7 \pm 0.3 \pm 1.9$	$19.6 \pm 0.7 \pm 0.7 \pm 0.6$
$D_0^*(2400)^-$	$12.1 \pm 0.8 \pm 0.3 \pm 0.6$	$13.1 \pm 1.0 \pm 0.8 \pm 0.5$
$D_2^*(2460)^-$	$1.31 \pm 0.04 \pm 0.02 \pm 0.02$	$1.31 \pm 0.04 \pm 0.04 \pm 0.00$
$D_3^*(2760)^-$	$0.053\,^{+0.011}_{-0.006} \pm 0.003 \pm 0.008$	$0.075\,^{+0.016}_{-0.008} \pm 0.005 \pm 0.003$

$$B^0 \to \overline{D}^0 \pi^+ \pi^-$$

Table 8: The phase of the complex coefficients of the resonant contributions for the Isobar model and the K-matrix model. The first uncertainty is statistical, the second and the third are experimental and model-dependent systematic uncertainties, respectively.

Resonance	Isobar $(\arg(c_i)^\circ)$	K-matrix $(\arg(c_i)^\circ)$
Nonresonance	$77.1 \pm 4.5 \pm 2.3 \pm 5.4$	n/a
$f_0(500)$	$38.4 \pm 2.7 \pm 1.3 \pm 3.7$	n/a
$f_0(980)$	$138.9 \pm 4.6 \pm 1.5 \pm 10.9$	n/a
$f_0(2020)$	$258.5 \pm 5.0 \pm 1.1 \pm 26.8$	n/a
$\rho(770)$	0.0 (fixed)	0.0 (fixed)
$\omega(782)$	$176.8 \pm 7.8 \pm 0.6 \pm 0.5$	$174.8 \pm 8.0 \pm 1.5 \pm 0.5$
$\rho(1450)$	$149.0 \pm 7.5 \pm 4.8 \pm 4.5$	$132.9 \pm 7.8 \pm 8.5 \pm 5.5$
$\rho(1700)$	$103.5 \pm 13.1 \pm 4.5 \pm 2.4$	$77.6 \pm 9.9 \pm 23.1 \pm 4.5$
$f_2(1270)$	$158.1 \pm 3.0 \pm 1.6 \pm 3.8$	$147.8 \pm 2.5 \pm 8.5 \pm 2.6$
$\overline{D}^0\pi^-$ P-wave	$266.7 \pm 3.7 \pm 0.3 \pm 7.1$	$261.0 \pm 4.0 \pm 3.3 \pm 6.7$
$D_0^*(2400)^-$	$83.6 \pm 4.4 \pm 2.8 \pm 4.6$	$78.4 \pm 4.1 \pm 11.5 \pm 1.7$
$D_2^*(2460)^-$	$262.9 \pm 2.9 \pm 0.8 \pm 3.0$	$257.4 \pm 3.4 \pm 0.7 \pm 1.9$
$D_3^*(2760)^-$	$91.1 \pm 6.7 \pm 1.4 \pm 5.1$	$92.7 \pm 7.3 \pm 15.2 \pm 2.3$

$B^0 \to \overline{D}^0\pi^+\pi^-$

Table 11: Measured branching fractions of $\mathcal{B}(B^0 \to rh_3) \times \mathcal{B}(r \to h_1h_2)$ for the Isobar and K-matrix models. The first uncertainty is statistical, the second the experimental systematic, the third the model-dependent systematic, and the fourth the uncertainty from the normalisation $B^0 \to D^*(2010)^-\pi^+$ channel.

Resonance	Isobar ($\times 10^{-5}$)	K-matrix ($\times 10^{-5}$)
$f_0(500)$	$11.2 \pm 0.8 \pm 0.5 \pm 2.1 \pm 0.5$	n/a
$f_0(980)$	$1.34 \pm 0.25 \pm 0.10 \pm 0.46 \pm 0.06$	n/a
$f_0(2020)$	$1.35 \pm 0.31 \pm 0.14 \pm 0.85 \pm 0.06$	n/a
S-wave	$14.1 \pm 0.5 \pm 0.6 \pm 1.3 \pm 0.7$	$14.2 \pm 0.6 \pm 1.5 \pm 0.9 \pm 0.7$
$\rho(770)$	$32.1 \pm 1.0 \pm 1.2 \pm 0.9 \pm 1.5$	$31.0 \pm 1.0 \pm 2.1 \pm 0.7 \pm 1.5$
$\omega(782)$	$0.42 \pm 0.11 \pm 0.02 \pm 0.03 \pm 0.02$	$0.43 \pm 0.11 \pm 0.02 \pm 0.02 \pm 0.02$
$\rho(1450)$	$1.36 \pm 0.28 \pm 0.08 \pm 0.19 \pm 0.06$	$1.91 \pm 0.37 \pm 0.73 \pm 0.19 \pm 0.09$
$\rho(1700)$	$0.33 \pm 0.11 \pm 0.06 \pm 0.05 \pm 0.02$	$0.73 \pm 0.18 \pm 0.53 \pm 0.10 \pm 0.03$
$f_2(1270)$	$9.5 \pm 0.5 \pm 0.4 \pm 1.0 \pm 0.4$	$9.1 \pm 0.6 \pm 0.8 \pm 0.5 \pm 0.4$
$D_0^*(2400)^-$	$7.7 \pm 0.5 \pm 0.3 \pm 0.3 \pm 0.4$	$8.0 \pm 0.5 \pm 0.8 \pm 0.4 \pm 0.4$
$D_2^*(2460)^-$	$24.4 \pm 0.7 \pm 1.0 \pm 0.4 \pm 1.2$	$23.8 \pm 0.7 \pm 1.2 \pm 0.5 \pm 1.1$
$D_3^*(2760)^-$	$1.03 \pm 0.16 \pm 0.07 \pm 0.08 \pm 0.05$	$1.34 \pm 0.19 \pm 0.16 \pm 0.06 \pm 0.06$

$$\mathcal{B}(B^0 \to \overline{D}^0\pi^+\pi^-) = (8.46 \pm 0.14 \pm 0.29 \pm 0.40) \times 10^{-4}$$

$$\mathcal{B}(B^0 \to \overline{D}^0\omega(782)) = (2.75 \pm 0.72 \pm 0.13 \pm 0.20 \pm 0.13^{+0.20}_{-0.23}) \times 10^{-4}$$

$$\mathcal{B}(B^0 \to \overline{D}^0 f_2(1270)) = (16.8 \pm 1.1 \pm 0.7 \pm 1.8 \pm 0.7^{+0.5}_{-0.2}) \times 10^{-5}$$

$B^0 \to \overline{D}^0 K^+ \pi^-$

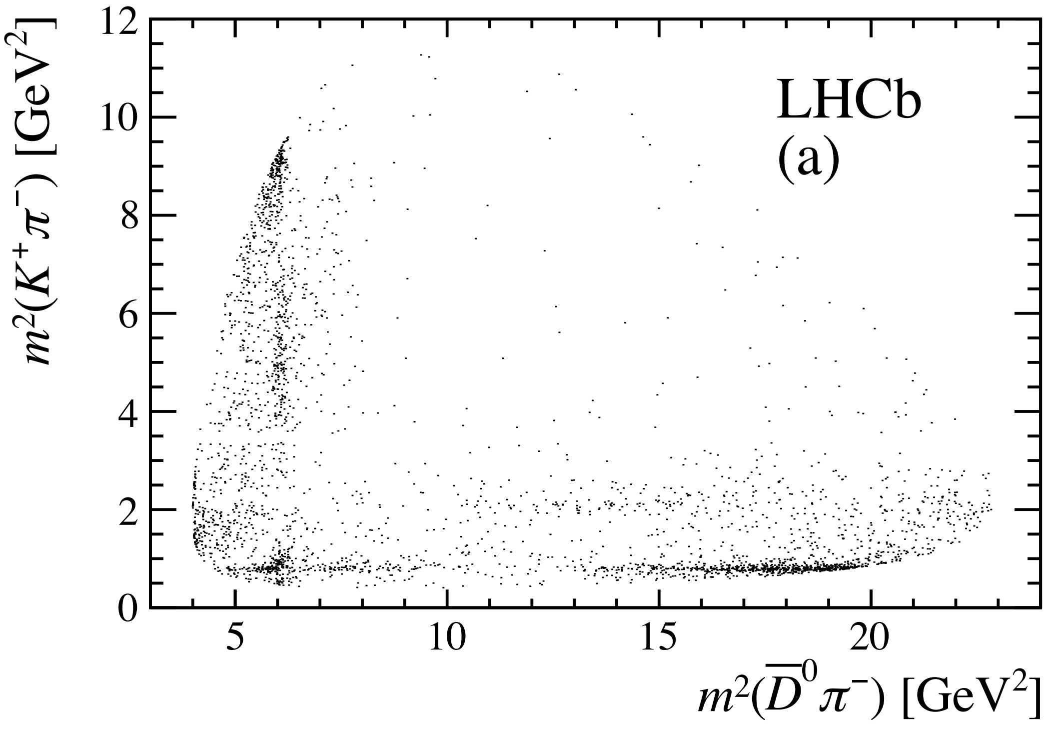

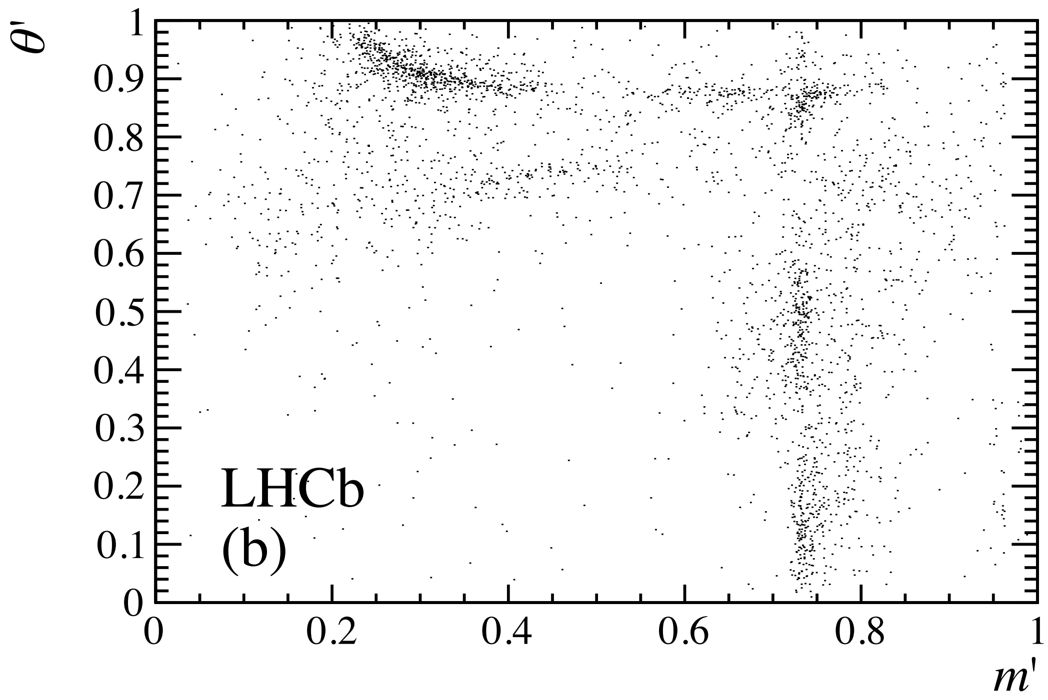

$$B^0 \to \overline{D}^0 K^+ \pi^-$$

The LASS lineshape [51] has been developed to combine these two contributions,

$$R(m) = \frac{m}{q \cot \delta_B - iq} + \exp\left[2i\delta_B\right] \frac{m_0 \Gamma_0 \frac{m_0}{q_0}}{(m_0^2 - m^2) - i m_0 \Gamma_0 \frac{q}{m} \frac{m_0}{q_0}}\,, \tag{8}$$

$$\text{where } \cot \delta_B = \frac{1}{aq} + \frac{1}{2} r q\,, \tag{9}$$

and where m_0 and Γ_0 are the pole mass and width of the $\overline{K}_0^*(1430)$ state, and a and r are shape parameters.

[51] J. Phys. G36 (2009) 075003

The $D\pi$ S-wave nonresonant contribution can be described by the "dabba" lineshape [52], defined as

$$R(m) = \frac{B'(m^2)(m^2 - s_A)\rho}{1 - \beta(m^2 - m_{\rm min}^2) - iB'(m^2)(m^2 - s_A)\rho}\,, \tag{10}$$

where

$$B'(m^2) = b \exp\left[-\alpha(m^2 - m_{\rm min}^2)\right]\,. \tag{11}$$

Here $m_{\rm min}$ is the invariant mass at threshold, $s_A = m_D^2 - 0.5\, m_\pi^2$ is the Adler zero, ρ is a phase-space factor and b, α and β are parameters with values fixed to $24.49\,{\rm GeV}^{-2}$, $0.1\,{\rm GeV}^{-2}$ and $0.1\,{\rm GeV}^{-2}$, respectively, according to Ref. [52].

[52] Nucl. Phys. B296 (1988) 493

$$B^0 \to \overline{D}^0 K^+ \pi^-$$

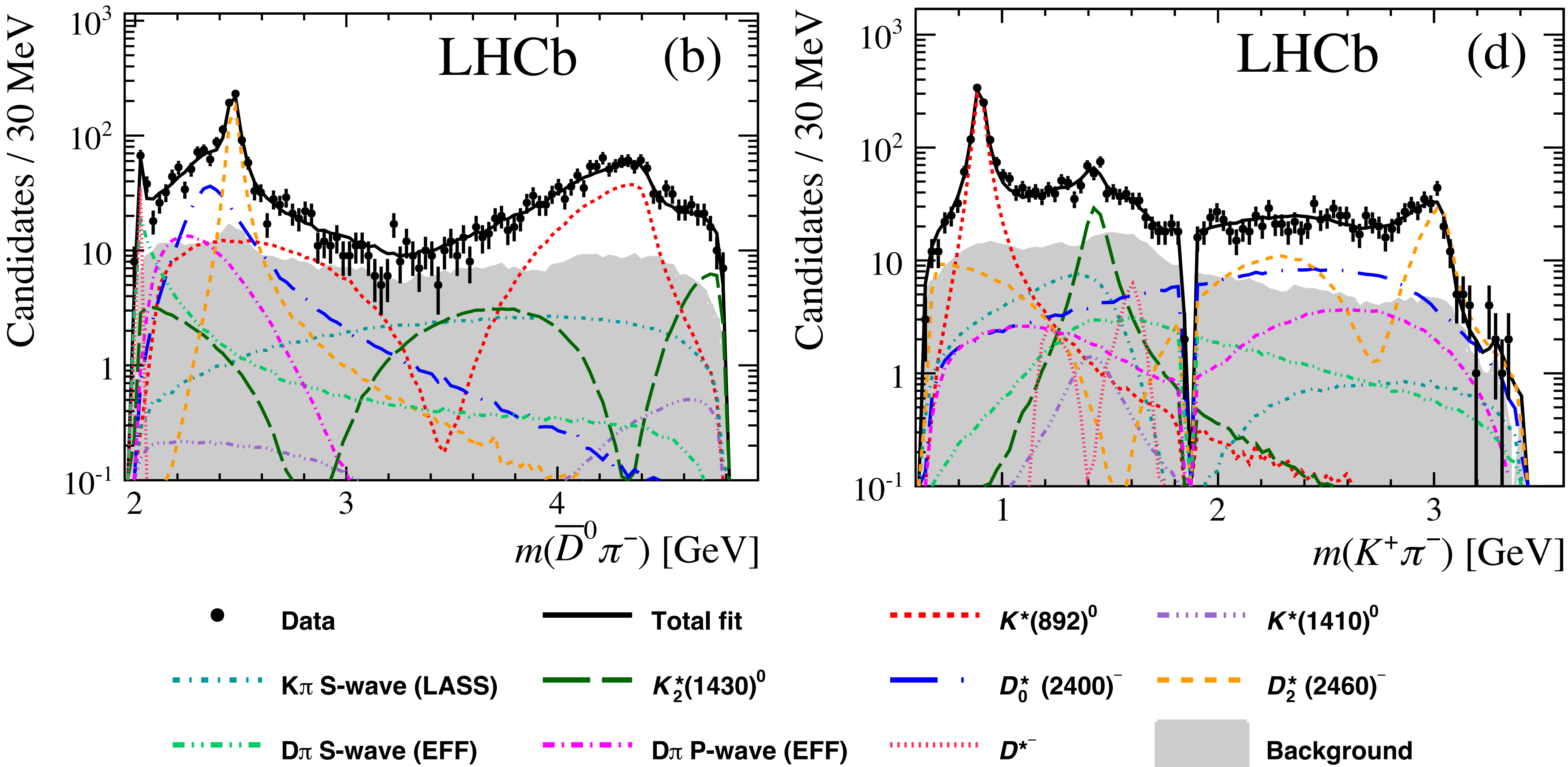

$B^0 \to \overline{D}^0 K^+ \pi^-$

Table 7: Results for the complex amplitudes and their uncertainties presented (top) in terms of real and imaginary parts and (bottom) in terms and magnitudes and phases. The three quoted errors are statistical, experimental systematic and model uncertainties, respectively.

Resonance	Real part	Imaginary part
$K^*(892)^0$	$-0.00 \pm 0.15 \pm 0.24 \pm 0.34$	$-1.27 \pm 0.06 \pm 0.03 \pm 0.06$
$K^*(1410)^0$	$0.15 \pm 0.06 \pm 0.04 \pm 0.09$	$-0.09 \pm 0.09 \pm 0.18 \pm 0.18$
$K_0^*(1430)^0$	$0.14 \pm 0.38 \pm 0.48 \pm 0.38$	$0.45 \pm 0.15 \pm 0.37 \pm 0.17$
LASS nonresonant	$-0.10 \pm 0.24 \pm 0.16 \pm 0.42$	$0.44 \pm 0.14 \pm 0.17 \pm 0.23$
$K_2^*(1430)^0$	$-0.32 \pm 0.09 \pm 0.15 \pm 0.23$	$-0.47 \pm 0.07 \pm 0.14 \pm 0.15$
$D_0^*(2400)^-$	$-0.80 \pm 0.08 \pm 0.07 \pm 0.22$	$-0.44 \pm 0.14 \pm 0.12 \pm 0.18$
$D_2^*(2460)^-$	1.00	0.00
$D\pi$ S-wave (dabba)	$-0.39 \pm 0.09 \pm 0.09 \pm 0.14$	$0.36 \pm 0.17 \pm 0.14 \pm 0.23$
$D\pi$ P-wave (EFF)	$-0.62 \pm 0.06 \pm 0.03 \pm 0.11$	$-0.03 \pm 0.06 \pm 0.05 \pm 0.10$

Resonance	Magnitude	Phase
$K^*(892)^0$	$1.27 \pm 0.06 \pm 0.03 \pm 0.05$	$-1.57 \pm 0.11 \pm 0.16 \pm 0.27$
$K^*(1410)^0$	$0.18 \pm 0.07 \pm 0.10 \pm 0.11$	$-0.54 \pm 0.21 \pm 0.55 \pm 1.04$
$K_0^*(1430)^0$	$0.47 \pm 0.09 \pm 0.10 \pm 0.14$	$1.27 \pm 0.95 \pm 1.04 \pm 0.81$
LASS nonresonant	$0.46 \pm 0.14 \pm 0.16 \pm 0.29$	$1.79 \pm 0.65 \pm 0.35 \pm 0.69$
$K_2^*(1430)^0$	$0.57 \pm 0.05 \pm 0.04 \pm 0.08$	$-2.16 \pm 0.19 \pm 0.43 \pm 0.43$
$D_0^*(2400)^-$	$0.91 \pm 0.07 \pm 0.06 \pm 0.17$	$-2.64 \pm 0.15 \pm 0.14 \pm 0.23$
$D_2^*(2460)^-$	1.00	0.00
$D\pi$ S-wave (dabba)	$0.53 \pm 0.07 \pm 0.04 \pm 0.14$	$2.40 \pm 0.27 \pm 0.24 \pm 0.44$
$D\pi$ P-wave (EFF)	$0.62 \pm 0.06 \pm 0.04 \pm 0.11$	$-3.09 \pm 0.10 \pm 0.07 \pm 0.17$

$$B^0 \to \overline{D}^0 K^+ \pi^-$$

Table 9: Results for the product branching fractions. The four quoted errors are statistical, experimental systematic, model and PDG uncertainties, respectively. Upper limits are given at 90 % (95 %) confidence level.

Resonance	Product branching fraction (10^{-5})	Upper limit (10^{-5})
$K^*(892)^0$	$3.42 \pm 0.13 \pm 0.10 \pm 0.16 \pm 0.40$	
$K^*(1410)^0$	$0.07 \pm 0.03 \pm 0.08 \pm 0.07 \pm 0.01$	< 0.29 (0.34)
$K_0^*(1430)^0$	$0.47 \pm 0.18 \pm 0.22 \pm 0.31 \pm 0.05$	
LASS nonresonant	$0.44 \pm 0.34 \pm 0.34 \pm 0.61 \pm 0.05$	
LASS total	$0.61 \pm 0.25 \pm 0.25 \pm 0.49 \pm 0.07$	
$K_2^*(1430)^0$	$0.68 \pm 0.15 \pm 0.10 \pm 0.18 \pm 0.08$	
$D_0^*(2400)^-$	$1.77 \pm 0.26 \pm 0.19 \pm 0.67 \pm 0.20$	
$D_2^*(2460)^-$	$2.12 \pm 0.10 \pm 0.11 \pm 0.11 \pm 0.25$	
$D_3^*(2760)^-$		< 0.10 (0.11)
$D\pi$ S-wave (dabba)	$0.60 \pm 0.13 \pm 0.11 \pm 0.34 \pm 0.07$	
$D\pi$ P-wave (EFF)	$0.81 \pm 0.15 \pm 0.20 \pm 0.27 \pm 0.09$	

Table 10: Results for the branching fractions. The four quoted errors are statistical, experimental systematic, model and PDG uncertainties, respectively. Upper limits are given at 90 % (95 %) confidence level.

Resonance	Branching fraction (10^{-5})	Upper limit (10^{-5})
$K^*(892)^0$	$5.13 \pm 0.20 \pm 0.15 \pm 0.24 \pm 0.60$	
$K^*(1410)^0$	$1.59 \pm 0.68 \pm 1.81 \pm 1.59 \pm 0.36$	< 6.7 (7.8)
$K_0^*(1430)^0$	$0.71 \pm 0.27 \pm 0.33 \pm 0.47 \pm 0.08$	
LASS nonresonant	$0.66 \pm 0.51 \pm 0.51 \pm 0.92 \pm 0.08$	
LASS total	$0.92 \pm 0.38 \pm 0.38 \pm 0.74 \pm 0.11$	
$K_2^*(1430)^0$	$2.04 \pm 0.45 \pm 0.30 \pm 0.54 \pm 0.25$	